https://doi.org/10.26682/sjuod.2023.26.2.13
Journal of University of Duhok., Vol. 26, No.2 (Pure and Engineering Sciences),Pp 145-167, 2023

APPLICATION OF DIGITAL IMAGE CORRELATION METHOD IN MATERIALS - TESTING AND MEASUREMENTS: A REVIEW

MERNA **A**LEC **Z**AYA, **S**ARHAT **M**. **A**DAM and **F**ARSAT **H**EETO **A**BDULRAHMAN
Dept. of Surveying Engineering, College of Engineering, University of Duhok, Kurdistan Region–Iraq

(Received: April 26, 2023; Accepted for Publication: July 27, 2023)

ABSTRACT

Digital image correlation **(DIC) is a non-contact optical approach that employs tracking and image registration techniques to evaluate image alterations within two or three dimensions precisely. The DIC approach's primary focus revolves around identifying similarities between images that have undergone deformation, commonly referred to as the "degraded image," and images that have remained unchanged, known as the "Reference image." This approach is utilized in diverse scientific and technical disciplines to measure full-field displacement and strains. DIC is widely recognized as a valuable and efficient technique for quantifying in-plane deformation. Moreover, DIC is currently being utilized to monitor the behavior of concrete before fractures, including the propagation and displacement of cracks. Additionally, new applications of DIC are continuously being discovered. This paper aims to review the various applications of DIC and compare its capabilities with conventional measurement techniques, such as gauges and transducers, in the context of material testing and deformation measurement.**

Keywords: Digital Image Correlation (DIC), strain, displacement, concrete cracks, concrete fracture.

1. INTRODUCTION

It has always been vital to measure displacements and displacement gradients (strains) by assessing material qualities, such as the strength or fracture parameters of material, or performing experimental stress analysis. Optically-based techniques such as speckle interferometry, moiré interferometry, and holography have succeeded in various applications (Hung & Voloshin, 2003). However, the stability of the system is critical for all interferometric methods. In addition, it takes a long time and effort to process fringe patterns. Scholars have devised automated processes to process the data generated by fringe patterns such as Digital Image Correlation (DIC) in response to this technical challenge (Hung & Voloshin, 2003).

In engineering and building projects, strain and displacement are crucial characteristics. However, monitoring these parameters outside the laboratory presents a strict trade-off between accuracy, simplicity, and expense (McCormick & Lord, 2010). Since DIC has the potential to be a simple, inexpensive, and accurate approach, it could be beneficial for researching fracture propagation and material deformation in practical applications.

When cracks appear on the concrete's surface, it is a warning sign that the structure is degrading, and therefore, it is essential to investigate the cause of these cracks. Although the crack inspection is most commonly performed by hand or visually, the drawing of the fracture and the conditions of the irregularities are noted during the manual check (Mohan & Poobal, 2018). Unfortunately, the manual approach needs more impartiality in quantitative analysis because it relies solely on the user's knowledge and expertise. Hence, this paper reviews an image-based crack detection system to replace manual inspection.

Determining the deformation of structures subjected to varying loads is critical and challenging since it is hard to obtain accurate data and expensive to use the necessary equipment (Gencturk, Hossain, Kapadia, Labib, & Mo, 2014). Strain gauges, linear variable differential transformers (LVDTs), and laser Doppler vibrometers have all been created to monitor surface deformation. Despite their high reliability and accuracy, they can only measure one dimension at a single place and require direct contact with the examined structures(J. J.

Wang, Gowripalan, Li, & Nguyen, 2019). The utilization of strain gauges and LVDTs for deformation distribution measurement (DDM), which requires simultaneous two dimensional (2D) and three dimensional (3D) measurements at multiple locations, is characterized by high costs and operational challenges. (Gencturk et al., 2014).

Due to recent technological advancements, measuring methods in several scientific domains have experienced substantial change, and DIC is one of them. It provides a wide range of capabilities compared to the prior and traditional approaches (Deng & Zhao, 2013; Gencturk et al., 2014; Biswal & Ramaswamy, 2016). With the advent of DIC, it is now possible to understand fracture dynamics comprehensively. Furthermore, it has proven to be a valuable tool in experimental mechanic's research (Xie, Zhou, Lu, & Chen, 2017).

DIC was created in the 1980s by a team of academics at the University of South Carolina (Peters & Ranson, 1982; Peters, Ranson, Sutton, Chu, & Anderson, 1983; Chu, Ranson, & Sutton, 1985; M. Sutton, Mingqi, Peters, Chao, & McNeill, 1986; M. A. Sutton, Orteu, & Schreier, 2009). In the last 30 years, DIC has been improved and widely employed in various sectors (Pan, Qian, Xie, & Asundi, 2009; Pan, 2011). The initial algorithm for digital image correlation utilizing the Fast Fourier Transform (FFT) technique was introduced by Sciammarella et al. in 1983. During the 1990s, DIC garnered increased attention as a result of the proliferation of high-performance computing systems and the advancement of more intricate algorithms. The enhancement in precision and reduction in computational time was achieved through the advancement of algorithms utilizing image intensity correlation, notably the Subset-based DIC (M. A. Sutton et al., 2009; Blaber, Adair, & Antoniou, 2015). During the 2000s, there was a significant increase in the adoption of DIC across multiple academic disciplines, such as materials science, mechanical engineering, and biomechanics. As a result of the growing prevalence of digital cameras and the advancement of high-speed imaging technology, techniques for DIC have undergone development to accommodate larger image datasets and facilitate high-speed motion analysis. In recent years, the field of DIC has made significant progress by incorporating 3D DIC techniques, enabling the quantification of deformations and strains in three-dimensional space. Scholars have also endeavored to integrate sophisticated image processing methodologies, such as image segmentation and feature tracking, to enhance the precision and effectiveness of DIC. The integration of DIC algorithms with additional imaging techniques, such as stereo imaging and digital volume correlation, has been employed to enhance the analysis of intricate deformation fields, resulting in a more comprehensive evaluation (Hosseinzadeh, 2020).

In addition, non-contact optical strain and displacement measurements can now be made with DIC. Many applications are feasible due to DIC's ease of use and low cost compared to other techniques, such as speckle interferometry. Also, it is more accurate and subjective than manual measurement techniques (McCormick & Lord, 2010). To operate DIC successfully, pixel blocks must be unique and random, with varying contrast and intensity levels (McCormick & Lord, 2010). When a structure or component's natural surface has a fine image texture, no additional surface preparation is needed for DIC (McCormick & Lord, 2010).

The DIC approach starts with a photograph taken before loading (reference image), followed by shots taken throughout the deformation process (distorted images). Each distorted image has a unique random dot pattern compared to the original, unreformed reference image. These discrepancies between patterns can be computed using computer software (GOM correlate, MATLAB, VIC, and DIC engine) by associating all the pixels in the reference image and any deformed image and then creating a strain distribution map (McCormick & Lord, 2012).

In general, three processes are involved in implementing DIC approaches for measuring shape, motion, and deformation. (1) Fabrication of speckle patterns: It provides a carrier for deformation information on the test sample surface. This phase, however, might be skipped if the sample surface has a changing intensity distribution with appropriate contrast; (2) Image capture: This method involves taking pictures of the test specimen's surface in different conditions with either a single camera, considered as two-dimensional DIC or two synchronized cameras, known as stereo-DIC; (3) Analyses of photos: Specifically, it employs a proprietary cross-correlation technique to compare distorted images to a reference image to resolve displacement and strain fields (Dong & Pan, 2017).

As a result, DIC measurements are impossible without a speckle pattern. A speckle pattern (i.e., the random gray intensity pattern) covering the surface of the specimen is required for accurate and consistent matching in the subsequent correlation computation. Speckle patterns can significantly affect the accuracy and precision of DIC displacement measurements and their essential role in DIC measurements. Numerous researchers (Zhou & Goodson, 2001; Lecompte et al., 2006; Yaofeng & Pang, 2007; Pan, Xie, Wang, Qian, & Wang, 2008) (Y. Wang, Sutton, Bruck, & Schreier, 2009; Pan, Lu, & Xie, 2010; Hua et al., 2011; Stoilov, Kavardzhikov, & Pashkouleva, 2012; Bossuyt, 2013; Crammond, Boyd, & Dulieu-Barton, 2013; X.-Y. Liu et al., 2015; Mazzoleni, Zappa, Matta, & Sutton, 2015; Neggers, Blaysat, Hoefnagels, & Geers, 2016; Bomarito, Hochhalter, Ruggles, & Cannon, 2017) have demonstrated that an increased number of gradients in a speckle pattern is advantageous, as resulted in fewer bias errors and fewer random errors.

To obtain accurate DIC measurements, a good speckle pattern must have particular qualities. The following characteristics should apply to the speckle pattern on the test sample's surface: (1) high contrast: Variable grayscale levels as well as relatively substantial intensity gradients; (2) isotropy: lack of pattern directionality. The pattern should lack any real directionality; and (3) randomness: a non-repeating, irregular pattern used to refine full-field displacement mapping (P. Reu, 2014b). (4) Stability: Good speckle patterns should be firmly adhered to the specimen's surface and distort together with the sample surface despite massive translation and deformation (P. Reu, 2014b, 2014a, 2015a, 2015b).

Displacement measurement accuracy and precision can be improved using the subpixel registration process. However, the classic forward additive Newton–Raphson (FA-NR) algorithm (Bruck, McNeill, Sutton, & Peters, 1989; Bing, Hui-Min, Bo-Qin, & Fu-Long, 2006; Pan & Li, 2011) and the more recent advanced inverse compositional Gauss-Newton (IC-GN) algorithm (Pan, Li, & Tong, 2013; Pan, 2014; Pan, Tian, & Song, 2016; Pan & Wang, 2016) were discovered to be preferred due to their higher accuracy, broader applicability, and better noise-proofing capabilities (J. Zhao, Sang, & Duan, 2019).

Correlation can be calculated if the surface texture distribution of the sample is natural and uniform, it is feasible to utilize the natural roughness of rocks, wood, soil, and large-scale constructed structures such as bridges for pattern matching in the monitoring of deformation (Hall et al., 2010; Bourcier, Bornert, Dimanov, Héripré, & Raphanel, 2013; Gauvin, Jullien, Doumalin, Dupré, & Gril, 2014). Macro-scale patterns are typically created using airbrushing and spraying. Therefore, spray bottles and airbrushes are commonly employed for pattern fabrication. The speckle size distribution and standard deviation can be influenced by several factors, including air pressure, solution viscosity, nozzle diameter, and distance from the substrate (Rayan, 2008; Lugli, 2009; Lionello & Cristofolini, 2014). To determine the parameters, a pre-experiment should be carried out.

The correlation criteria used in DIC to compare the intensity patterns of the reference and target subsets, are examined and divided into four types to help users understand their mathematical definitions and reciprocal interactions. They are insensitive to the distorted image's variations in offset and scale. Hence the ZNCC, ZNSSD, and PSSDab criteria with two extra unknown parameters are recommended for practical application. Their transversal linkages are proven mathematically and verified by computer simulation and experiments. The three correlation criteria are comparable, allowing for elegant pattern matching. Compared to other correlation criteria, the PSSDab criterion with two more unknown factors is slightly faster (Pan, Xie, & Wang, 2010).

Digital Image Correlation (DIC) offers significant advantages in non-contact measurement, particularly when compared to foil gauges. Unlike foil gauges, which only measure strain in a specific region, DIC can measure strain in all regions captured by the photographed images. Additionally, DIC surpasses strain gauges in terms of durability, as the latter are susceptible to breakage during testing. In contrast, DIC can be seamlessly conducted throughout the entire testing process.

To follow, this paper aims to review the aspects of DIC used in materials testing and measurements and the available work that DIC has been utilized to compare with conventional measuring tools.

2. STRAIN MEASUREMENT USING DIC

Strains have a role in various critical material properties and parameters (e.g., the stress-strain curve, Poisson's Ratio, and Young's Modulus). Strain can be defined in any material as the product of the change in length and the original length (Williams, 2001). Recently, new and more sophisticated research has necessitated strain measurements at any location inside an area of interest better understanding material and structural component behavior. As a result, researchers are interested in a strain map covering the entire surface. Unfortunately, specific conventional strain measurement instruments (e.g., strain gauge and LVDT) are inaccessible to create strain maps due to their high cost and impracticality (Cintrón & Saouma, 2008). Due to the requirement for strain maps to conduct new investigations, DIC is a new method developed to achieve these desired outcomes. In addition, it generates a contour map of the strains on the whole surface of a specimen subjected to mechanical testing.

Diverse studies on the implementation of DIC to observe strains and displacement in the domains of concrete structures have been undertaken (Gencturk et al., 2014; P. Zhao, Zsaki, & Nokken, 2018; Huang et al., 2019; Ottman et al., 2019). This breakthrough has been made possible by adapting, calibrating, and improving the DIC (Baldi & Bertolino, 2015),(Lehoucq, Reu, & Turner, 2015; Sebastian & Patterson, 2015) through its use on various materials and under a variety of situations (Y. Liu et al., 2015; Seo, Kim, Park, & Jung, 2015). Additionally, it enables the observation of the evolution of fracture openings (Verbruggen, Aggelis, Tysmans, & Wastiels, 2014); Caggegi, Sciuto, and Cuomo (2018). Thus, the determination of errors caused by picture distortion as an effect of the DIC experimental equipment has been explored and improved (Gao, Zhang, Su, & Wu, 2017; Y. Su, Gao, Zhang, & Wu, 2018; Y. Su et al., 2019).

Full-field evaluations are one of its key advantages, as demonstrated in (Ramos, Braga, Eslami, Tavares, & Moreira, 2015) study. They used a Tee Rosette strain gauge to measure strain in two perpendicular directions. DIC images were taken for each test step after stopping the hydraulic machine; the LVDT analog signals (load/displacement) and approach for tensile properties. INSTRON load cell are synchronized with the strain gauge's real-time (xxx/yyy) strain recording. DIC applications must speckle the test specimen randomly. The correlated solutions Vic-3DTM system was used to gather and analyze pictures for DIC analysis. The two 4.1MP complementary metal-oxide-semiconductor (CMOS)s cameras were positioned 1800 mm apart, with an aperture angle of roughly 27°. For more details about such a test, the reader can find (Ramos et al., 2015).

The DIC approach has received increased attention because of its wide range of potential uses, such as strain and displacement mapping. Wherein research by (Quanjin, Rejab, Halim, Merzuki, & Darus, 2020), three different materials have been tested. The analysis methods used include experimental, strain gauge, and DIC. The American Society for Testing and Materials (ASTM) D638 specifies the specimen's structural dimension. The top crosshead loading rate was set to 1 mm/min following ASTM 638. The Nikon D3100 camera captured the tensile test video at 4608 x 3072 pixels (14.2 effective megapixels). The resolution of the images can be increased to zoom into the specimen to improve strain accuracy and spatial resolution (P. L. Reu et al., 2018). Preparing the testing specimen requires spraying the surface with a black or white background before applying the speckles (M.-N. Su, Young, & Gardner, 2016). For reliable DIC findings, the speckle pattern should be filled with many black specks of varying sizes (Lecompte et al., 2006; Hua et al., 2011). Fig. **(*1*** demonstrates the graph of the stress-strain diagram of a glass fiber-reinforced plastic material subjected to tensile loading and measured using three different methodologies (experimental, strain gauge, and DIC).

Tensile loading caused the DIC Ncorr software to produce the contour plot image. Fig. **(*2*** depicts a contour plot of measured strain under tensile loading, including the analysis type, RG-DIC radius, step analysis, image correspondences, units/pixels, and correlation coefficient. The DIC approach was an acceptable alternative to the other two methods (experimental and strain gauges) regarding methodological considerations. Furthermore, it exhibits a reasonable agreement with experimental data, making it a simple evaluation

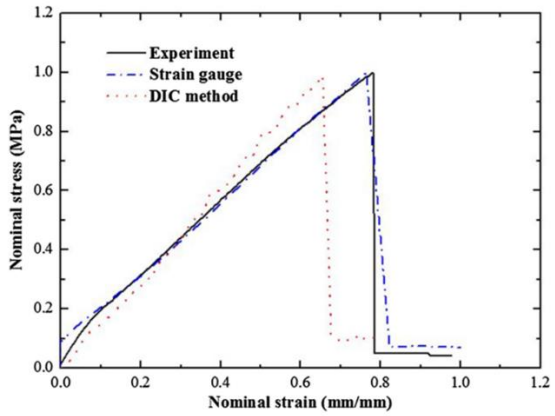

Fig. (1): Stress-strain graph of the glass-fiber-reinforced plastic material during a tensile test (Quanjin et al., 2020)

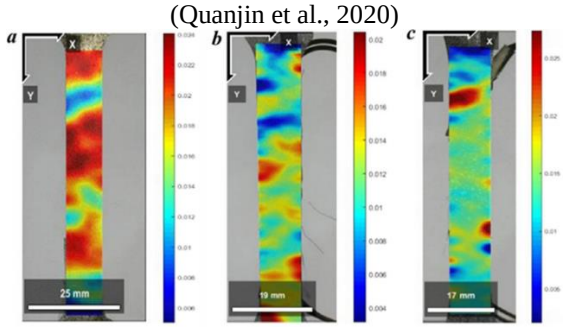

Fig. (2): Image of DIC method under applied tensile loading, a) Aluminum, b) glass fiber reinforced plastic, c) pure resin plastic (Quanjin et al., 2020)

Furthermore, several studies have demonstrated the convenience and efficiency of utilizing the DIC method for conducting uniform tension tests. For instance, Hung and Voloshin (2003) conducted a stress test by machining a dog-bone-shaped specimen from an aluminum plate to ensure consistent uniaxial stress. In (Hung & Voloshin, 2003) study, the specimen's length was 115 millimeters, and its cross-sectional area was 28 mm². Three strain gauges were attached to one side of the specimen, each having an angle of 0, 45, and 90 degrees about the loading axis. Random paint created a speckled pattern on the specimen's other side. The sample was placed in an INSTRON 1011 for testing. The speckled pattern and strain gauges' readings were recorded throughout the loading history. Images from the test show two prominent marks on the speckled surface, one on each side of the loading axis. There were two makers roughly 400 pixels apart, so it was feasible to assess how much strain there was by comparing their relative positions. Newton-Raphson and DIC algorithms correlated five discrete picture subsets from the reference and distorted images. The measured data were smoothed using a linear regression method. The suggested algorithm's fundamental flaws were also examined when comparing two speckled patterns. The strain gauge readings from 0.0029 to 0.046 agreed with the tensile test results recorded with DIC.

In agreement with that, True strain at any specimen location may be measured with DIC, whereas the standard approach obtains the average strain. Additionally, it may be used to analyze the necking process accurately. The fracture strain is significantly more than the total elongation as determined by the conventional approach applied in (PI, Smith, Gothekar, & Chen, 2010) study, where a 2D deformation setup was required to quantify sheet metal strain (i.e., only one camera is needed). (PI et al., 2010) aimed to obtain consistent strain readings across the test region, so a high-speed camera and DIC system were placed on a tripod in front of the specimen. The DIC method utilized a correlation approach to measure the deformation, contour, and strain after the object was deformed. The camera was attached to a Windows XP Pro PC with a 2.13 GHz CPU, 2GB RAM, and ISTRA 4D software from Dantec Dynamic. The camera was set to 25 frames per second at a resolution of 1280×1024. Three points were chosen on the material by (PI et al., 2010) to compare DIC with conventional methods. A & C are the extensometer's two ends. As a result of necking, the strain levels at these two locations are found to be close to those obtained by an extensometer but somewhat lower. Point B indicates that the necking region is much larger than the extensometer data. Fig. **(3** demonstrates the strain vs. time. The results show, DIC can measure genuine strain wherever in the specimen, while the old approach measures average strain. Therefore, DIC can accurately analyze necking. The fracture strain was found to be substantially higher than the overall elongation.

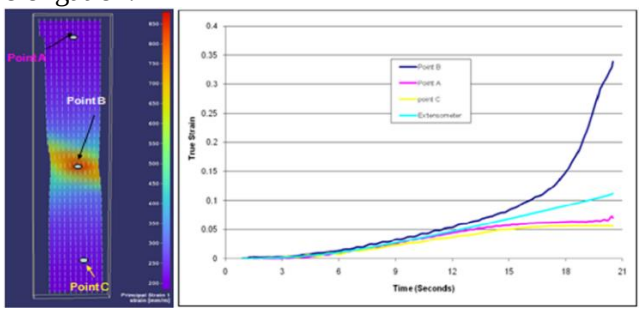

Fig. (3): Strain vs time profile with DIC and extensometer (PI et al., 2010)

On the other hand, the DIC technique has been used with other materials rather than aluminum steel and fiber-reinforced plastic. For example, DIC was employed to quantify strain variation in fiber-reinforced polymer confined concrete (Bisby, Take, & Caspary, 2007). This investigation aimed to directly compare hoop and axial strain recorded with foil strain gauges and digital image correlation. Three unwrapped and three fiber-reinforced polymers (FRP-confined) standard-sized unreinforced normal-strength concrete cylinders were tested in concentric, monotonic, uniaxial compression. They were wrapped in one layer of a commercially available hand lay-up carbon fiber reinforced polymers (CFRP) strengthening system in the hoop direction. The FRP system).

The structural performance of heat-damaged reinforced concrete columns wrapped with CFRP can be studied using DIC. As in the study of (Y. S. AL-KAMAKI, AL-MAHAIDI, & BENNETTS, 2017), concrete columns were prepared and burned, to imitate real-world circumstances. Some columns were unwrapped, while others have been repaired with one or two CFRP sheets. The DIC system took high-resolution photos of the concrete column's surface during mechanical testing. These cameras captured load-induced column deformation. Camera photos were analyzed using advanced image processing techniques. Digital Image Correlation accurately measured strain distribution on column surfaces. The DIC system allowed researchers to measure strain differences along column height throughout different loading stages till failure showed significant strain fluctuations throughout column height, notably for heat-damaged CFRP-wrapped columns. CFRP-confined columns had lower lateral strains than CFRP coupons in direct tensile tests, indicating lower strain efficiency. The DIC system provided essential strain distribution and CFRP strengthening data for heat-damaged concrete columns. It enabled the researchers to draw conclusions about the behavior of the repaired columns and supported the use of CFRP as a reliable material for structural strengthening.

In some cases, the discrepancy in strain gauges and DIC results can occur due to the erroneous placement of examined point in the specimen. As shown in the results of (Coșa, Hegheș, Negruțiu, & Kiss, 2020) experiment, A strain gauge with an accuracy of 0.001 mm was utilized to measure the strain readings of concrete at midspan. In addition, LVDT displacement sensors were employed to monitor provider advised a 100 mm hoop overlap in all circumstances. Digital images of the cylinder were taken every five seconds till failure using a Canon digital rebel camera featuring an 8-megapixel sensor. The geoPIV program employed normalized cross-correlation to define and track certain regions of interest in the first image. Using the geoPIV code (White, Take, & Bolton, 2003), the measurement precision is often better than 1/10th of a pixel. Using geoPIV, digital image correlation can accurately estimate axial strains and hoop strains (as well as strain variation) in FRP-constrained concrete cylinders. Strains recorded with the new technique correlate well with those obtained with conventional foil strain gauges, as shown in (

the deflection at midspan. The DIC approach was used to assess half of each beam, where a digital camera (NIKON D3100, 14.2-megapixel DX-format F-mount camera) and computer software (GOM Correlate 2016) for image processing were used to implement the optical technique (DIC). As determined by the DIC technique, the ultimate strain in the longitudinal reinforcement was roughly 70% lower than the strains obtained with strain gauges. When measuring concrete strains at the beam's top, the DIC technique provided findings comparable to those of a conventional extensometer. As previous studies have found, the utilized 2D camera to acquire the images may also introduce errors in the correlation, such as lens distortion. Fig. **(4** depicts the strains measured with the DIC technique and assessed with the GOM Correlate 2016 software.

DIC enables the determination of the distribution of surface strains rather than depending on single location measurements, as would be the case with strain gauges (Y. S. S. Al-Kamaki, 2021). This deformation can be gained by employing 3-dimensional DIC employing Vic-3D software to analyze pictures of a surface to detect pixel variance, which is then utilized to create strain contour maps rather than relying on strain gauges. DIC permits the determination of surface strain distribution.

LVDTs are used with strain gauges for accurate strain and displacement measurements. They have also been used in tests comparing the DIC technique to assess the reliability of the DIC as a replacement for LVDTs. The DIC methodology is a valid and accurate measurement method for full-scale concrete testing compared to data obtained using conventional LVDT instruments. Even at deficient strain levels, the DIC approach provided a significant advantage because it could

identify the load routes by interpreting the strain fields (less than the concrete cracking strain of approximately 0.00008). However, the measurement area's illumination considerably influences the accuracy of the results. An external light source must ensure that the area of interest is consistently illuminated, as the internal ambient light is insufficient. Only a somewhat constant illumination level is required for low measurement noise; moreover, the amount of illumination is less significant than keeping the illumination level constant across the entire measuring region.

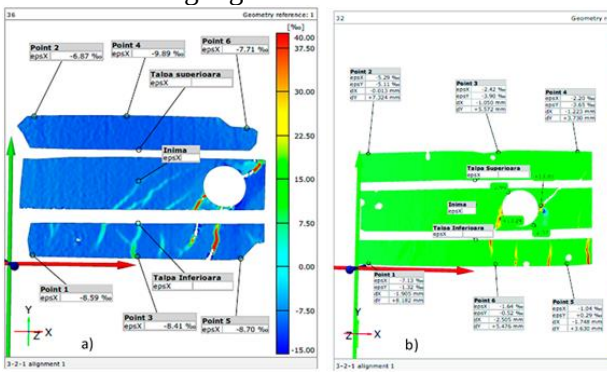

Fig. (4 a): Strains evaluated experimentally utilizing the digital image correlation approach for fly ash beams , b) Strains evaluated experimentally utilizing the digital image correlation approach for limestone beams (Coșa et al., 2020)

Regarding the applied speckle pattern to the surfaces of specimens, the size and distribution of black dots and their contrast with the background significantly affect the measurement's reliability. This effect was shown in an experiment by (Gencturk et al., 2014), testing a 7.62 m long, 711.2 mm deep I-beam.

APPLICATION OF DIC IN CRACK DEVELOPMENT AND PROPAGATION MONITORING

Concrete, mortar, and masonry are quasi-brittle materials requiring extensive crack behavior tests to fully understand their structural behavior.

Image-based measurements can extract information about cracks from structural surfaces. Using contactless instrumentation can reduce the impact on the test setup. There are two ways to measure cracks using images: directly and indirectly. Direct image-based crack measurements employ methods of image processing that vary the brightness of greyscale or color pixels. On the other hand, Indirect measures are based on DIC findings. Correlating the subsets of pixels allows for recording the spatial changes between the original and the distorted states of the pixels (array of neighboring pixels). As image-based measuring technology depends on sensor resolution and area of interest, both techniques require high-resolution cameras to record accurate crack patterns (Gehri, Mata-Falcón, & Kaufmann, 2020).

The beam was loaded vertically to its sheer capacity during testing using a steel loading frame and a 2.7 MN (600 kips) hydraulic actuator. LVDTs were used to measure the beam displacements in the failure zones close to the load application points. On the North and Southeast sides of the beam, six LVDTs were installed in a rosette to monitor average deformations. In order to compare strain data from traditional measurement devices with the DIC system, the DIC-based non-contact measurement system was installed on both the North and Southwest sides of the beam. For non-contact DIC measurements, cameras with 50 mm fixed focal lenses and a high-performance computer are utilized. Furthermore, an additional light source was installed to illuminate the measuring surface. LVDTs were used on both sides of the beam to collect data. **Error! Reference source not found.** compares average compression diagonal strains recorded by LVDTs (ND1 and SD1) and computed by DIC. Comparing the East and west Sides of the beam shows good agreement. Similarly, the average tension diagonal strains detected by LVDTs (ND2 and SD2) and computed by DIC are shown in **Error! Reference source not found.**. The results of (Gencturk et al., 2014) 's test show good correlations between the two methods and proved the DIC technique's suitability for monitoring complex deformations in pre-stressed concrete elements.

Additionally, DIC provides information that would otherwise be unavailable (

Table (1): Details and Results of the preliminary testing program (Bisby et al., 2007)

Name	FRP²	Axial Strength (MPa)	Strengthening ratio	Ult. Axial strain (foil)%	Ult. Axial Strain(photo)%	Ult. Axial strain (foil)%	Ult. Axial Strain(photo)%	Strain efficiency(foil)%	Strain efficiency(photo)%
0-1	None	33.30	0.960		0.360		-0.280		
0-2	None	35.50	1.020		0.300		-0.150		
0-3	None	34.40	0.990		0.330		-0.250		
1-1	1-ply	44.10	1.270	0.820	0.800	-0.980	-0.930	0.760	0.720
1-2	1-ply	44.10	1.270	0.930	0.870	-1.040	-1.100	0.810	0.850
1-3	1-ply	43.00	1.240	0.910	0.900	-0.950	-1.210	0.740	0.940

Table (*2*). It measures the average strain along the whole specimen, excluding gripping regions, indicating clamping slippage relative to the integrated transducer, unaffected by fractures or local strain concentrations. Stress distribution in dry fiber bundles might be examined. DIC provided fracture counts, their locations, widths, and lengths while testing composites. After the test, the fracture pattern is used to choose measurement regions, so that the dependability of the specimen as a whole is unaffected by the precise placement of any cracks. Maximum virtual markers can be set without adding time or expense. Finally, DIC is non-contact; hence it poses no harm to equipment and is less affected by conventional transducers' stroke or weight (Tekieli, De Santis, de Felice, Kwiecień, & Roscini, 2017).

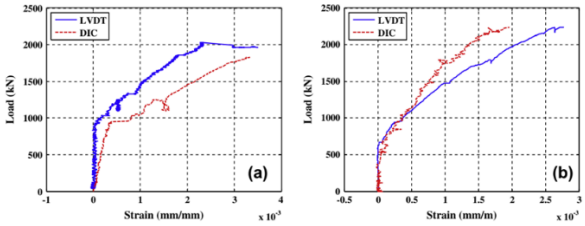

Figure 5 Comparison of average compression and tension diagonal strains at the a) Northern and b) Southern ends of the beam (Gencturk et al., 2014)

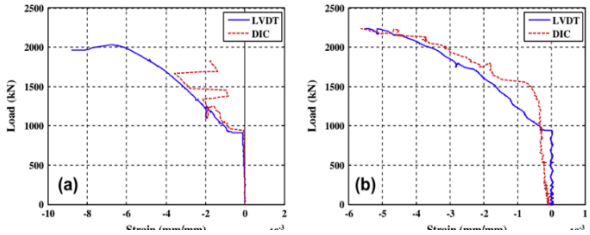

Fig. (6): Comparison of average tension diagonal strains at the a) Northern and b) Southern ends of the beam (Gencturk et al., 2014).

3. APPLICATION OF DIC IN CRACK DEVELOPMENT AND PROPAGATION MONITORING

Concrete, mortar, and masonry are quasi-brittle materials requiring extensive crack behavior tests to fully understand their structural behavior.

Image-based measurements can extract information about cracks from structural surfaces. Using contactless instrumentation can reduce the impact on the test setup. There are two ways to measure cracks using images: directly and indirectly. Direct image-based crack measurements employ methods of image processing that vary the brightness of greyscale or color pixels. On the other hand, Indirect measures are based on DIC findings. Correlating the subsets of pixels allows for recording the spatial changes between the original and the distorted states of the pixels (array of neighboring pixels). As image-based measuring technology depends on sensor resolution and area of interest, both techniques require high-resolution cameras to record accurate crack patterns (Gehri, Mata-Falcón, & Kaufmann, 2020).

Table (1): Details and Results of the preliminary testing program (Bisby et al., 2007)

Name	FRP²	Axial	Strengtheni	Ult.	Ult.	Ult.	Ult.	Strain	Strain

		Strength (MPa)	ng ratio	Axial strain (foil)%	Axial Strain(photo)%	Axial strain (foil)%	Axial Strain(photo)%	efficiency(foil)%	efficiency(photo)%
0-1	None	33.30	0.960		0.360		-0.280		
0-2	None	35.50	1.020		0.300		-0.150		
0-3	None	34.40	0.990		0.330		-0.250		
1-1	1-ply	44.10	1.270	0.820	0.800	-0.980	-0.930	0.760	0.720
1-2	1-ply	44.10	1.270	0.930	0.870	-1.040	-1.100	0.810	0.850
1-3	1-ply	43.00	1.240	0.910	0.900	-0.950	-1.210	0.740	0.940

Table (2): Comparison of traditional sensors with DIC (Tekieli et al., 2017)

Test	Aim	traditional procedures/sensors limit	DIC limitations and potentialities
Dry textile specimen tensile testing	Global (average) and local strains, as well as the tensile modulus of elasticity	The built-in transducer of the examination device • • Unreliable in the occurrence of textile slippage in the gripping regions Extensometer • inappropriate application (especially on steel cords) • • Unreliable when the cord/yarn it is tied to has ruptured • • Affected on a modest scale by potential strain concentrations • • The application process is challenging and time-prolonged (particularly on steel wires). • Very localized value	Potentialities • Slippage in the gripping sections does not affect the overall measure. • • Capability to identify the strain of every yarn (if just one or two markers are inserted per yarn) • Strain variations in individual yarns may be detected.
Tensile tests on composite specimens (FRP/SRP as well as FRCM/SRG)	Global (average) and local strains evaluation, as well as the tensile modulus of elasticity.	The built-in transducer of the examination device • Extensometer is unreliable in the event of gripping area slippage. • Affects by the position of the cracks • Complex application on large cross-section specimens	Potentialities • Slippage in the gripping sections does not affect the overall measure. • Based on the crack pattern, several measurement locations can be chosen to determine strain once the test is completed. Limits • There is no direct information on the textile in the matrix.
Shear bond tests on reinforced FRP/SRP and FRPU/SRPU composites	Detection and assessment of strain profiles along the bonded area.	Strain gauges • Application is difficult and time-consuming. • Localized value	Potentialities • On the bonded area, the strain field can be identified • The unequal distribution of strains and the concentrations of various strains can be identified.
Tests of shear bonding on FRCM/SRG reinforcements	Identifying and evaluating strain patterns across the bonded region.	Strain gauges • Application is difficult and time-consuming. • Localized value	Potentialities • Transducer encumbrance is not a concern. • Non-responsive to misalignments in the setup Limits • Fabric and reinforcement-to-substrate contact strain cannot be accurately detected. Not relevant in this context.

As mentioned above, A DIC-based method was introduced for automated crack detection and measurement (ACDM). The main concepts and processes of the ACDM procedure are illustrated in Figure 7. The instrumentation on the specimen's surface tracks full-field displacements using DIC. The crack identification algorithm uses the principal tensile surface strain field calculated from the collected data. Cracks are found in regions when the strain is above a specific level. Morphological thinning extracts crack structures as thinned lines associated with skeletons. Even at a strain threshold one order more extensive than the material's maximum elastic tensile strain, the crack detector shows good performance

compared to actual crack patterns. For example, cracks with a minimum opening of 0.05 px (or approximately 0.02 mm for an image resolution of 0.38 mm/px, which can be produced in a 2 m field of view with the DIC equipment described herein) are detectable. A direct image-based crack detection technology can identify a crack opening 100 times smaller than this. However, there are many advantages of using DIC-based methods, such as the extraction of more precise and accurate cracks (Gehri et al., 2020).

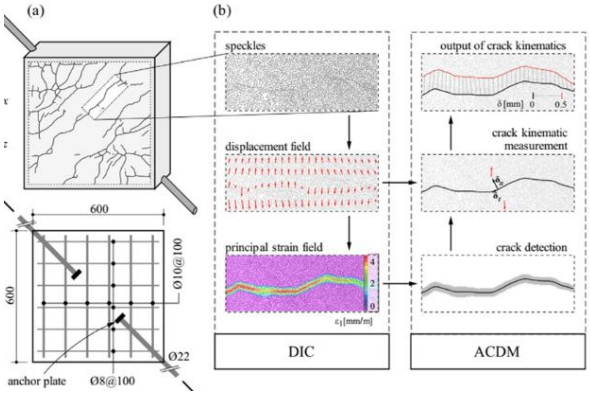

Fig. (7): The automatic crack identification and kinematic measuring technique is conceptualized as follows: (a) Experimental setup of structural concrete, including the crack pattern observed; (b) flowchart of the (ACDM) (Gehri et al., 2020)

Using the DIC method, the fracture characteristics of reinforced concrete may be observed and measured. When paired with a high-resolution camera, the DIC method proved an excellent tool for tracking the spread of cracks. However, traditional surface crack characterization methods still need to be more time-intensive and vulnerable to human error. Typically, crack characterization is performed visually using magnifiers or crack width rulers, as reported by (Fayyad & Lees, 2017). They used a digital single-lens reflex (DSLR) camera with a 35-megapixel CMOS sensor to capture photos of loaded test specimens. The tripod-held camera was at a right angle to the object. The camera featured a range of 24–120 mm focal length. Although the out-of-plane movement was not anticipated, the camera was placed 1,000 mm distant from the specimen's surface to decrease the impact of any such movement as recommended by (Hoult, Take, Lee, & Dutton, 2013). The camera's optical axis is perpendicular to the center of the sample or specimen. Depending on the beam's dimensions, the spatial resolution of various regions of interest varies. In this configuration, one pixel corresponds to approximately 30 nanometers on the surface of the beam on identical beams, where (Fayyad & Lees, 2017) deployed a second DSLR camera to improve the fracture process zone resolution and to record the fracture propagation on the opposite side of the investigated beam. External lighting was concentrated on the area to increase the image quality. Throughout this experiment, photographs were shot constantly every 10 seconds. According to the findings, the outcomes of DIC analysis are dependent on picture search patch size, length resolution, and search patch center distance. Depending on the issue being studied, different-sized search patches, length resolutions, and inter-patch distances needed to be tried to determine the optimal values for these factors.

Laboratory testing is critical to accurately characterizing a specimen's response to stress. In most cases, this is done with hand-drawn images. Therefore, a tool that can automatically detect, map, and measure crack patterns would be of primary significance. Because of recent technological advancements, digital optical devices and techniques have grown beyond their initial scope of use. Laboratory test monitoring is unquestionably one of these exciting new frontiers that have recently emerged (JMDA Valença, Dias-da-Costa, & Júlio, 2012). In addition, the method can be used to track the progression of cracks over time. The flowing steps of the process are as follows, (JMDA Valença et al., 2012):

Step 1: Priming the surface of the specimen with white paint to enhance how the cracks appear and set crack width rulers (CWR) to achieve more precise pictures.

Step 2: The image was captured with a low-cost digital camera orthogonally to the object's surface to minimize image distortion when utilizing a single image technique (Granshaw, 1980; J Valença, Júlio, & Araújo, 2012).

Step 3: Employs a global region of interest (GROI) to obtain high precision; A binary image is created for each stage, enhancing the surface discontinuities of the specimen.

Step 4: After analyzing the step 2 output for the phase of failure (which is anticipated to have the most significant cracks), the user selects ROIs for further analysis. Every stage in the worldwide cracking pattern can be documented.

Further, a Global Analysis defines the essential areas of the specimen. The global surface is then examined to get the whole crack pattern and characterize its progression.

Compared to past procedures, such as drawing the fracture pattern with crack magnifying lenses or CRW, 'MCRACK' offers considerable speed, efficiency, comprehensiveness, and dependability improvements. The method's biggest flaw is the user's selection of regions. MCRACK is a non-contact, low-cost measurement approach that does not need the use of professional cameras or previous familiarity with data processing.

4. CONCRETE FRACTURE MEASUREMENT USING DIC

DIC technique can assess anywhere along the fracture for crack opening displacement (COD), and it is comparable to the clip gauge in terms of accuracy (Xie et al., 2017). In addition, the fracture extension length can be easily obtained by DIC, which is not easily obtainable by other techniques. This method can be seen in the study of (Xie et al., 2017) utilizing digital image correlation technology to investigate the fracture behavior of geopolymer concrete. Low calcium fly ash was used to produce a geopolymer binder in this study. In addition, it has been discovered that Ground Granulated Blast Furnace Slag (GGBFS) increases the workability and regulates the setting of Geopolymer concrete (GPC) manufactured from fly ash (Zhuang et al., 2016). After 28 days of curing, the specimens were tested for fracture. Fig. **(8**a shows three-point bending tests done on single-edge notched beam specimens to assess the fracture characteristics of GPC produced with fly ash. Initially, the area around the notch tip was chosen as the DIC monitoring target, and a speckle pattern (sprayed black paint on a white background) was placed on the lateral surface of the beam specimen. The load-induced deformation of the specimen beam was then captured by two digital cameras placed in front of the beam. The distance between the camera and the beam was set to compromise the digital camera's field of view and the size of the region of interest (ROI).

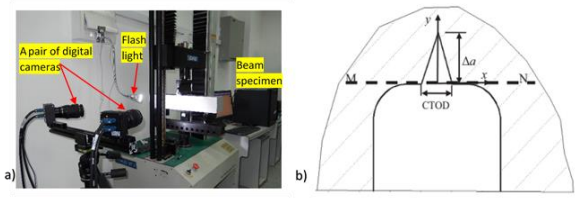

Fig. (8 a): The DIC measurement system's layout, b) schematic diagram of the crack tip (Xie et al., 2017)

A flashlight illuminated the beam specimen and reduced motion blur when capturing fast motion. The flashlight was angled slightly downward before the beam specimen to prevent glare on the digital cameras. The load produced by the Universal Testing Machine (UTM) was provided as an external parameter to the DIC measurement system to keep the load and deformation in sync. DIC permits the measurement of the beam specimen's 3D displacements and strains, enabling the estimation of additional fracture parameters. Fig. **(8**b illustrates the crack tip schematic. Crack opening displacement is depicted in the crack mouth opening diagram (CMOD) and the crack tip opening diagram (CTOD). The CMOD/CTOD may be determined from the DIC horizontal displacement field by drawing a horizontal line across the mouth or tip of the notch. For each fracture line segment, the horizontal displacements are averaged to determine the mean horizontal displacement of the crack. With increasing notch depth, the peak load of the beam specimens decreases while the peak load CMOD increases. DIC was utilized to examine the fracture behavior of GPC containing fly ash. Three-point bending studies were conducted on single-edge notched beam specimens with varying notch depths. DIC constantly monitored the displacement field of the beam. Midspan deflection, fracture extension length, CTOD, and CMOD were calculated using the measured displacement field. The linear elastic fracture mechanics theory computed the fracture energy and toughness. DIC can replace traditional measuring techniques in fracture tip monitoring. At any point along the fracture, COD can be measured. Clip gauge and DIC COD measurement precision are equivalent. DIC can get the fracture extension length relatively quickly, which is not easily obtainable with other techniques.

In reinforced concrete constructions, micro and macro cracks can grow simultaneously, making the fracture process more challenging (Fayyad & Lees, 2014). A range of elements, including strain localization, concrete heterogeneity, crack bridging, and the type of reinforcing, can all affect fracture behavior. Using the DIC approach, the fracture characteristics of reinforced concrete could be observed and quantified. Small-scale reinforced concrete beams can be monitored using the highly effective DIC method. For the objective of studying the influence of various parameters

of reinforced concrete beams, DIC was used to calculate the CMOD. As is apparent in the study (Fayyad & Lees, 2014), DIC fracture behavior was investigated by fabricating and testing two sets of reinforced concrete beams. Each set consists of seven beams, which share the exact dimensions and loads but have different reinforcement to concrete weight ratios and surface finishes. Photographs of the test samples of (Fayyad & Lees, 2014) were taken with a DSLR camera. Raising the camera's resolution improves the accuracy of measurements since displacement errors are measured in pixels. The resolution of the camera used in this test was 5472 by 3648 pixels, which is more than the resolution of the camera used in tests by (Wattrisse, Chrysochoos, Muracciole, & Némoz-Gaillard, 2001; Syed, Saliba, & Loukili, 2013; Dutton, Take, & Hoult, 2014). In the test of (Fayyad & Lees, 2014) a tripod was utilized to secure the camera, having an axis perpendicular to the subject. The lens was a standard 55 mm. Although the out-of-plane movement was not predicted in this testing, The camera was repositioned distant from the subject surface to reduce its effect as recommended by (Hoult et al., 2013). GeoPIV software was used to evaluate photos of each specimen under various loading situations. The displacement vectors derived from the DIC analysis findings were utilized to compute the CMOD values for the specimens that were evaluated. The CMOD values acquired by DIC were compared to the C-clip gauge results in Fig. **(*9*a.

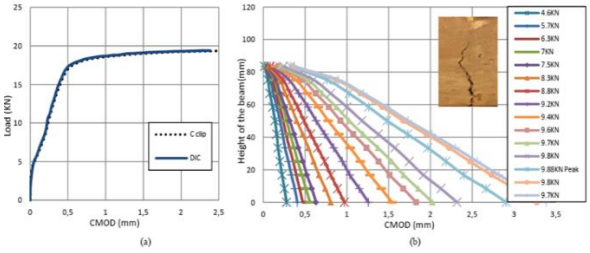

Fig. (9): DIC results in a)CMOD and c-slip b) crack propagation (Fayyad & Lees, 2014)

Fig. **(*9* b displays the CMOD values for beams M1, 0.5, FD, and 10, where the two graphs coincide. This match shows that the DIC technique employed measures the CMOD well. The surface displacements revealed scattering up to 50% of the peak load, indicating micro-cracks rather than macro cracks. The DIC method visualized and quantified fracture characteristics of reinforced concrete. The DIC approach works well for monitoring crack profiles in small reinforced concrete beams.

To accurately analyze concrete crack propagation behavior, it is necessary to accurately quantify the fracture process zone (FPZ), particularly the location of the crack tip.

Therefore, concrete fatigue and fracture performance research rely heavily on reliable measurements of crack tip location and FPZ. The DIC method can accurately detect the slightest displacement shift to detect the specific location of the concrete fracture tip, which was obtained by (Li et al., 2020). Three-point bending under static loading was used to acquire the concrete properties. The V-notch fracture specimen size (length/width/height): 450 mm, 150 mm, and 150 mm for the V-notch fracture. The prefabricated V-notch fracture with an angle of fewer than 15 degrees was shaped using a steel plate 5 mm thick and pointed at one end. The 0.001 mm/s displacement mode static loading was applied. The Materials Testing System (MTS) automatically measured the experimental load (P) and deflection. The CMOD was determined by positioning two knife edges and a COD extensometer on either side of the constructed notch. The strain variation was monitored by attaching two strain gauges (10 mm gauge length) to the tangent of the fracture tip of the prefabricated sample. The MTS machine and the concrete samples were photographed using a pair of charge-coupled device (CCD) cameras, as in Fig. **(*10* b. The camera acquisition frequency was 1 Hz in this test.

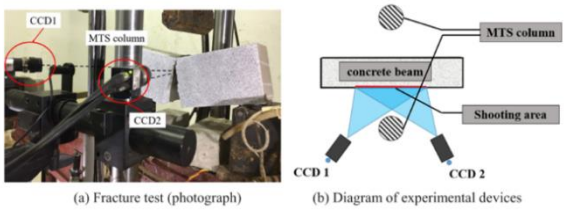

Fig. (10): Testing system of concrete fracture a) Fracture test photograph , b) Diagram of experiment devices (Li et al., 2020)

Without physically touching the beams, researchers could track the fracturing progress of the concrete using 3D DIC technology. Both strain and displacement fields were calculated using the commercial PMLABTM program. Following image acquisition, correlation calculations and displacement program

reconstruction were applied. Initial segment line y = 0 was taken from the tangential direction of the prefabricated fracture tip in the computation area. Then, for every 20 pixels, a segment line perpendicular to the height direction was defined.

Given that the three-point bending beam fracture is a mode I problem, the main focus is displacing the crack opening direction. Fig. (***11*** shows the DIC-derived strain and displacement fields for stage P1. The specimen's loadbearing capability was 3.99k in P1.

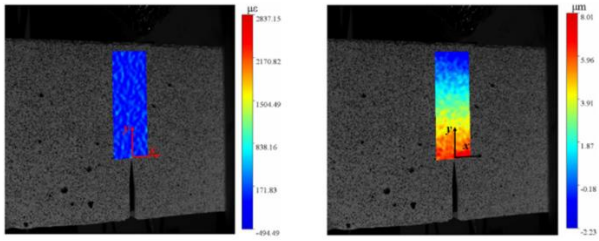

(a) Strain field (με) (b) Displacement field (μm)

Fig. (11 a): Stain field, b) Displacement field (Li et al., 2020)

A comparison of CMOD acquired by DIC and COD gauge is shown in Fig. (***12***. it has been demonstrated that DIC may be used effectively and reliably in concrete to detect fracture planes' crack tip location and size.

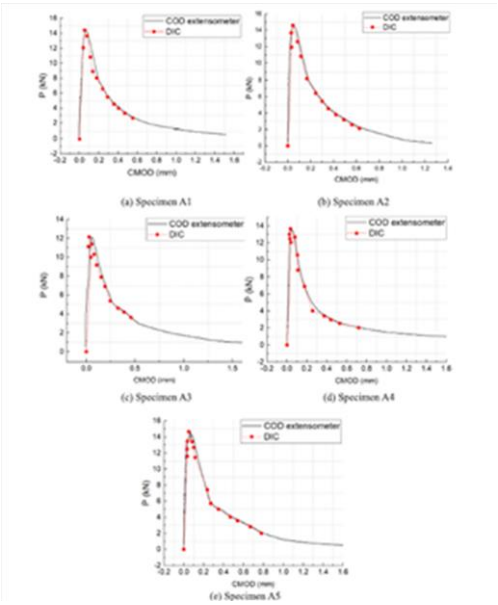

Fig. (12): A comparison of the CMOD values obtained using the DIC and COD gauges for a) specimen A1, b) specimen A2, c) specimen A3, d) specimen A4, e) specimen A5 (Li et al., 2020)

Two and three-dimensional cracks can be estimated using the DIC. It can be used to observe the testing of various specimen sizes under various loading circumstances; this was demonstrated in (Shah & Kishen, 2011), where a linear variable displacement transformer measured the load-point displacement, and on the notch, a clip gauge measured the CMOD. All tests were controlled using CMOD at 0.0005 mm/s crack opening. Digital images of the interface specimen were captured before and during loading using a digital camera affixed to the platform. Images were captured with remote control to eliminate camera shake and maintain an identical distance between the camera lens and the specimen being photographed. An algorithm by Eberl (Eberl, Thompson, Gianola, & Bundschuh, 2006) initially built-in MATLAB was used to correlate the digital images obtained during the experiments for each specimen. Analysis was carried out using a 512 x 512-pixel window with a pixel density of 4 pixels per millimeter. A square grid of 25 pixels (zone of interest) in each direction from the center grid region was used to calculate displacements and stresses. Fig. (***13***a illustrates the strain distribution, horizontal displacements from the DIC, and crack pattern observed during the test. The profile of horizontal displacement matches the crack pattern of the specimen.

On the other hand, Fig. (***13*** b depicts a three-dimensional deformation profile during loading. This graphic depicts the crack opening progressing during the test with the growing image number. This test is displayed in Fig. (***14***, together with the vertical load. The vertical displacements estimated by DIC and those measured empirically by an LVDT are shown to be quite similar, asserting the DIC technique's effectiveness.

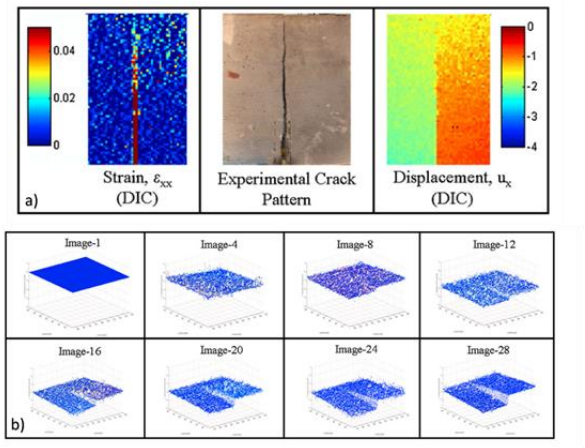

Fig. (13 a): Strain, crack pattern, and displacement measurements results, b) three-dimensional representation of displacement at various loading phases (Shah & Kishen, 2011)

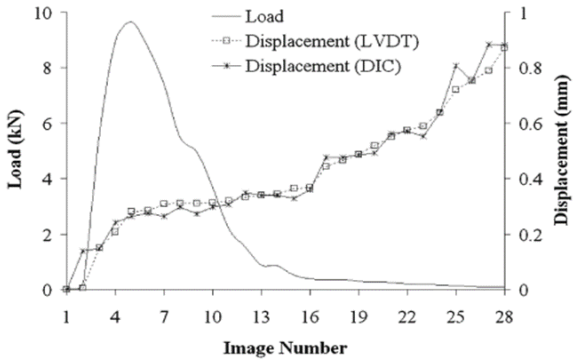

Fig. (14): Load vs. mid-span vertical displacement (interface beam AB) (Shah & Kishen, 2011)

DIC can be an effective and cost-effective alternative to strain gauges, slip gauges, and (LVDTs). Furthermore, DIC techniques allow accurate fracture tip and crack length measurements, which are difficult and expensive to achieve with standard sensors on concrete-like materials.

5. APPLICATION OF DIC IN DISPLACEMENT MEASUREMENT

Experimental solid mechanics depends on accurate displacement measurements of materials and structures exposed to a variety of loads (thermal or mechanical loading). Non-homogeneous material behavior cannot be evaluated using conventional strain measurement equipment, such as strain gauges, transducers, and LVDTs, which generally offer mean values of strains or displacements at selected places. Whole deformation field measurement approaches for composite materials have been proposed throughout the past decade (Grediac, 2004). An automated method for calculating surface strain and displacement was proposed in the 1980s utilizing DIC (Chu et al., 1985; Ranson, Sutton, & Peters, 1987; Bruck et al., 1989). Analog photogrammetry and vision metrology are viable alternatives to target localization in digital or digitized images (Van Den Heuvel, Kroon, & Le Poole, 1993).

Along with advanced DIC systems, Digital cameras can give reliable information when compared with LVDTs and strain gauges to measure strain and displacement. A strain measuring test on concrete was conducted (Aghlara & Tahir, 2018) using a standard digital camera; throughout the test, the specimen's face was photographed. The displacement of a specific spot-on concrete was recorded using an LVDT to produce a reliable criterion for correlation analysis results in the computer-controlled camera and took digital photos. The LVDT findings were recorded every 10 seconds to meet the DIC analysis criteria. The displacement findings of two DIC software for the exact location (Fig. (***15***) are virtually equal, with a difference of around 0.2 mm. After analysis, the desired displacements and stresses were determined for each image's ROI. Some of the critical aspects of this technology were observed: The suggested measurement method has an average accuracy of over 93% in determining specimen displacements, and ordinary cameras can give truthful results compared to conventional displacement measurement tools.

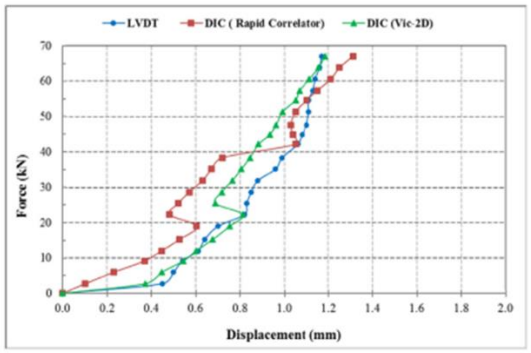

Fig. (15): Displacement of a single spot-on concrete in the specimen due to force (Aghlara & Tahir, 2018)

In agreement with these findings, another test was applied by utilizing a digital camera to study the displacement of materials using a sandstone sample. The researchers (Shukla & Mishra, 2018) experimented using a 60-tonne dynamic/static rock testing unit, and the sandstone was put through its paces in compression. A 0.5kN/sec loading rate was maintained. A SONY RX100 V digital camera with two stand lights focused on the specimen was used to take a series of photos. Displacement changes in image measurements are delivered in x, and y directions, (Figure 16). Because this was a compression test, the tallest peak is depicted, pointing toward y.

It was found that Digital Image Correlation is very accurate and can be utilized over and over again until the sample fail.

DIC was also used for full-field measurements of the fracture kinematics of prestressed concrete beams. A study by (Lakavath, Joshi, & Prakash, 2019) indicated that DIC is an appropriate tool for full-field computations. The critical shear crack may be traced throughout time using full-field displacement measurements.

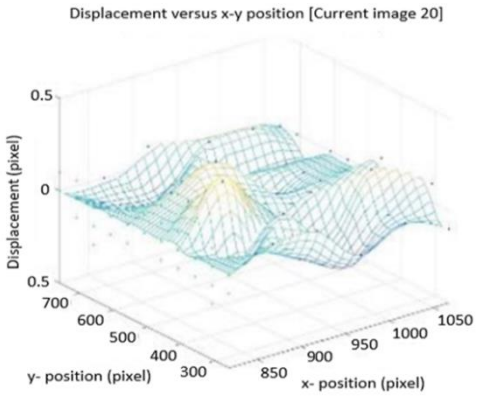

Fig. (16): The deformed image's displacement in the X and Y axes (Shukla & Mishra, 2018)

Search patches and search patch distance can significantly affect the resolution of the images. Surface displacements are extremely sensitive to the search patch size of images since they are considered as very small values. Obviously, the higher the image length resolution, the better the accuracy obtained (Tejchman, 2010; Skarżyński, Syroka, & Tejchman, 2011; Skarżyński, Kozicki, & Tejchman, 2013). According to Fig. **(17**, Using a high resolution of 90 pixels/mm, the distance between search patch center pixels of 15 pixels, a confined zone of horizontal displacement, and normal horizontal strain above the beam notch can be observed at maximum load.

When utilizing the experimental program (Kozicki & Tejchman, 2007) and commercial software (Correlated Solutions, 2009), the measured displacements in Fig. **(17** are identical for varied search patch sizes (Correlated Solutions, 2009).

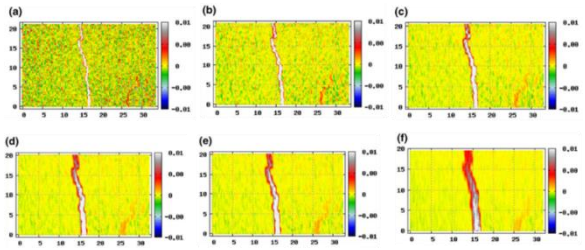

Fig. (17): Experiments with a fine-grained concrete notched beam, 'A1', localized zones just above the notch at peak load based on horizontal normal strain computed utilizing own software, with a high length resolution of 90 pixels/mm and a search patch distance of 15 pixels at various search patch sizes: 30 pixels (a), 60 pixels (b), 90 pixels (c), 120 pixels (d), 150 pixels (e), and 180 pixels (f) The vertical and horizontal axes represent coordinates in millimeters, and color scale strain intensity (Skarżyński et al., 2013)

The practice of 3D-DIC is remarkable in displacement measurements, which involve utilizing unique systems such as ARAMIS. For example, in (Boulekbache, Hamrat, Chemrouk, & Amziane, 2015), Both cameras in the system had a maximum frame rate of 7 Hz and a resolution of 2048 by 2048 pixels. They were placed 535 mm apart from the sample and 400 mm apart from one another as shown in Fig. ***(18***. In addition, LVDTs positioned on the specimen's second side adhered to the specimen to measure the specimen's transverse displacement (i.e., displacement perpendicular to the plane of loading).

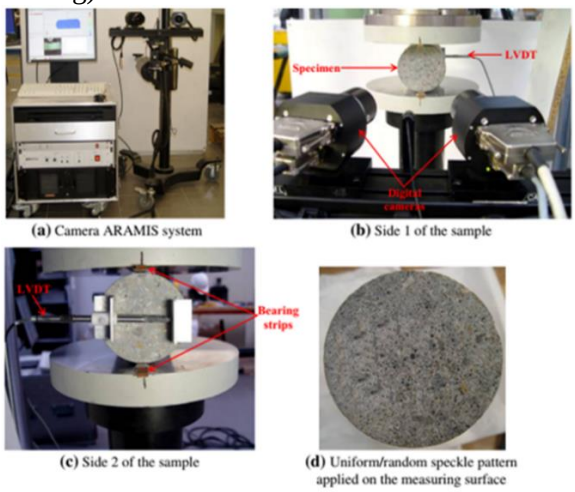

Fig. (18): Tensile splitting test a) Camera Aramis system , b) Side 1 of the sample , c) Side 2 of the sample , d) Uniform/ random speckle pattern applied on the measuring surface (Boulekbache et al., 2015)

Comparing LVDT and DIC-Aramis data for a single sample (FRSCC35-1) reveals a reasonable correlation (Fig. ***(19)***). A strong correlation between the two methods confirms the DIC's method reliability for measuring deformation.

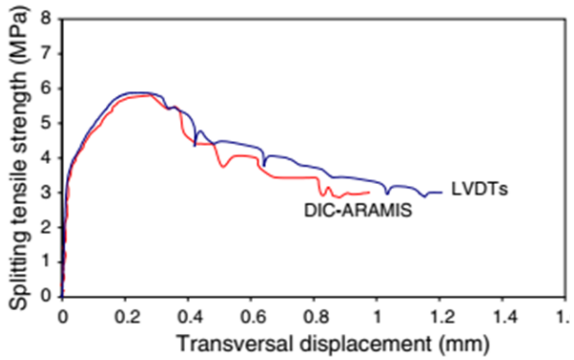

Fig. (19): LVDT and DIC-ARAMIS transverse displacement comparison (Boulekbache et al., 2015)

DIC approaches can also benefit from using video records and photographs taken at regular intervals, as shown in (Pérez, Prieto, & Orduz, 2021) where NIKON D5600 digital SLR camera and 18–55mm lens was utilized for that purpose. Each test used the same light source, an LED Yn-300 III Youngnuo light, to maintain a consistent black-to-white contrast over the ROI as recommended by (Bigger et al., 2018). At 1.40 m from the ROI, the camera and light source were mounted at the same height as the specimen, using a tripod to ensure a stable set-up. **Error! Reference source not found.** displays the reference scales used to calibrate and scale the displacement readings appropriately. Another stochastic pattern was placed close to the actuator to calibrate the parameters, subset, and distance between subsets, as shown in **Error! Reference source not found.**. The camera video mode, which provided a 1920 x 1080 pixels' spatial resolution, was used to capture the displacement images. However, the effective resolution over the ROI was roughly 1235 x 410 pixels, with a conversion ratio of 0.3 mm/pixel. Photos were taken from the videos every five seconds to collect the displacement data for each load increase recognized by the system. For the specimens M1(a) and M7(a), the Ncorr® v1.2 software-generated displacement fields in the y-direction, (**Error! Reference source not found.** b).

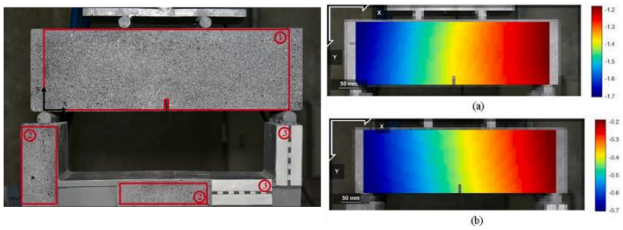

Fig. (20): FPBT. Left photo, set-up 1) ROI 2) reference pattern 3) reference scale (1 unit = 1 cm), Right photo, Displacement in Y direction of 2 samples, (a) for M1, (b) for M7 (Pérez, Prieto et al. 2021)

CMOD can be measured with CMOD gauges and compared to the results of DIC in measuring CMOD, digital images were continually captured during a load` test in an experiment by (Alam, Loukili, & Grondin, 2012). The beam was photographed using two digital cameras with macro lenses of 75 mm; The digital cameras have 256 grayscale levels with a resolution of 1040 x 1392 pixels. There were two sets of experiments, one for each beam size. Cameras were mounted to capture a 60x100-millimeter section of the beam in the first series. The notched opening and the first fracture profile were recorded at this position. One pixel in the image corresponds to a 35 μm square on the specimen, which is adequate to estimate displacement measurements with an accuracy of two μm. (Corr, Accardi, Graham-Brady, & Shah, 2007). The three-point bending tests were carried out with the assistance of closed-loop universal testing equipment that had a capacity of 160 kN. Because of the uneven surface, a circular jack was utilized to apply the weight.

The correlation approach is used to find each subpixel in the imaging region. The appropriate displacement vectors along the coordinate axis are indicated. Horizontal (axial) displacement may be determined from the horizontal (axial) displacement vectors. **Error! Reference source not found.**(a) depicts the beam's axial displacement field (specimen D2 at maximum load). Before the notch, displacement values show a noticeable rise, indicating a crack in the material. The crack path may be determined using this figure. The opening displacement of the notch mouth was measured with a CMOD gauge and compared to that value (**Error! Reference source not found.**B).

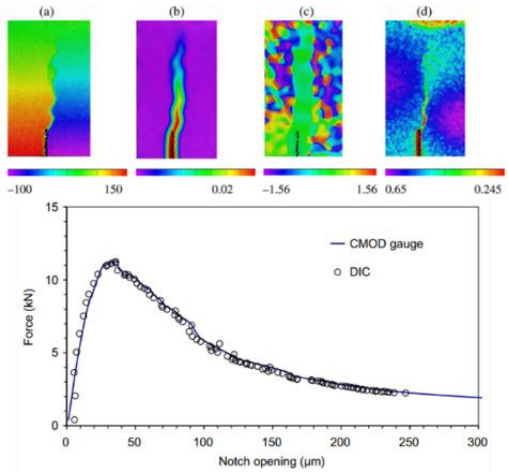

Fig. (21): Top) Displacement and strain of D2 at peak load a) axial displacement b)green langrage strain c) principal strain direction D) correlation error, bottom) force-notch mouth opening displacement curve of D2 beam using CMOD gauge and DIC (Alam et al., 2012)

The highest difference between the two readings is three μm, indicating good agreement between the two methods. However, since the DIC method can only give surface fracture readings, some differences may occur due to the material's anisotropy.

A conclusion can be drawn based on the research reviewed on tested materials: digital image correlation can be used to characterize materials; However, some factors must be considered to prevent the acquisition of erroneous displacement measurements. Variations in light intensity during picture acquisition, specimen accommodation movements out of the plane, pattern quality, and image resolution impacted the calculations during the test. The significant advantage of the approach was its capacity to determine the fracture process in the splitting. According to the findings, the DIC method has the potential to produce exceptional accuracy and a comprehensive data.

The deformation of road materials under various load circumstances is assessed using the Digital DIC approach. The study of (Górszczyk, Malicki, & Zych, 2019) made use of AC11S hot-mix asphalt (HMA), often known as asphalt concrete. Additionally, geosynthetic materials such as triaxial hexagonal polypropylene geogrid, biaxial polyester fiber geogrid, and biaxial glass fiber geogrid were employed. The result of this research showed that along with the solution of the principal strain values and principal directions, it was capable of determining displacements and deformations in any direction and at any point (for the whole surface of the sample).

6. DISCUSSION AND CONCLUSION

By reviewing previous studies concerning DIC, many advantages of image processing-based measurements were found, including:

(1) the reduced labor required; (2) the rapid capture of large amounts of geometric data through the use of images; and (3) the ability to return to visual records and perform future further analysis. From the papers reviewed, it was clear that Strain gauges and (DIC) capacity to conduct full-field assessments are in good agreement, proving that DIC is a practical and reliable structural health monitoring tool. DIC compares the subject alterations due to various forces to the changes in the original body. It can measure the parameter down to the nanometer scale, resulting in more accurate results. Mechanical devices, such as contact-based mechanisms, frequently have poor outcomes because of the material heterogeneity, immunity to noise, etc. Repeating experiments is also less reliable, resulting in the waste of sensors. A real-time displacement measurement system based on digital image processing techniques is novel, cost-effective, and simple to install while still retaining the benefits of dynamic measurements with high resolution. As a result, it is envisaged that this technique will give the sensing and tracking community a significant addition to the current list of sensor technologies.

According to the findings of this study, it can be stated that this method is capable of measuring and examining strain at the concrete surface and has advantages over conventional methods. The followings are some of the most notable aspects of this method:

1) It is possible to simultaneously measure the bond strain in all of its components on a concrete surface using the 2D-DIC approach.

2) During loading, 2D-DIC can show the exact behavior of bond strain at the concrete surface and its growth on the specimen.

3) Non-contact DIC can measure all the strain components on all specimen points in the form of a full-filled distribution at any loading step, unlike conventional methods that can only be applied to a single spot.

4) The suggested measurement method has an average accuracy of more than 93% in estimating specimen displacements.

5) Using the 2D-DIC approach to map the full-field distribution of strains can assist one in forecasting the cracking zone on concrete before failure occurs.

The accuracy of strain readings has been determined to be within ±200μ when compared to strain gauge data in normal circumstances by utilizing a camera fixed on a tripod, use oriented, and equipped with conventional lenses.

Speckle patterns and targets can be easily created for most common investigations from millimeters up to meters in scale. However, speckle pattern quality assessment and production could be a significant challenge for the practitioner because of the wide range of test materials, spatial scales, and experimental settings.

Photogrammetric approaches employing the DIC method allow for the determination of the nature of the work on the entire surface of the tested element, allowing for the determination of the most demanding areas and deformations of composite and concrete. Before creating the diagonal crack, the DIC approach allows researchers to predict the appearance of the crack path and track it throughout the research. The capacity to detect load paths (through strain field interpretation) even at deficient strain levels was regarded as the most advantageous extra feature of the DIC technique (less than the concrete cracking strain of approximately 8.0×10^{-5}. Other limitations were sensitive to the light source and a random speckle pattern, the inability of conventional algorithms to identify cracks or report their widths, and loss of data in regions where abnormally extensive fractures and spalling cover the concrete. A good fact is that before the specimen shows cracks, the axial strain map can show the areas where the cracks will appear in the specimen. A high-quality measurement depends on determining the cause of the mistake and the estimation rate. Testing and analytical errors are the two most common sources of mistakes in the DIC procedure. However, because only the specimens outside the surface are being monitored, no specific information on the textile within the matrix is available.

However, the disadvantage of employing DIC is data loss in locations where significant cracks and/or spalling of concrete are detected. In addition, more information is needed on the distance variation between the ROI and the DIC system. The DIC system's reliance on natural lighting conditions and the necessity of employing artificial light for capturing high-frequency images. It is imperative to utilize calibration tables that are suitable for the dimensions of the tested sample area, as well as storage media with sufficient space to archive recorded images and acquire research outcomes.

RECOMMENDATION FOR FURTHER STUDIES

In favor of DIC and material testing concerns, this study recommends more investigation into the type of cameras used in the image acquisition stage and the ability to utilize low-cost cameras and mobile cameras for data collection. Also, more studies are recommended to investigate the safest ground sampling distance between the camera and the specimen when the test is in progress. Furthermore, it is suggested to examine the photo acquisition mode employed by mobile phone cameras and their capacity to capture the motion of speckle patterns throughout the entire loading process of the sample.

REFERENCES

Aghlara, R., & Tahir, M. M. (2018). Measurement of strain on concrete using an ordinary digital camera. *Measurement, 126*, 398-404. doi:https://doi.org/10.1016/j.measurement.2018.05.066

AL-KAMAKI, Y. S., AL-MAHAIDI, R., & BENNETTS, I. (2017). STRAIN EFFICIENCY OF CARBON FIBRE REINFORCED POLYMER-CONFINED RC COLUMNS. *Journal of Duhok University*, 484-497. doi:https://doi.org/10.26682/sjuod.2017.20.1.43

Al-Kamaki, Y. S. S. (2021). Ultimate strain models derived using a Digital Image Correlation (DIC) system for preloaded RC columns subjected to heating and cooling and confined with CFRP sheets. *Journal of Building Engineering, 41*, 102306. doi:https://doi.org/10.1016/j.jobe.2021.102306

Alam, S., Loukili, A., & Grondin, F. (2012). Monitoring size effect on crack opening in concrete by digital image correlation. *European journal of environmental and civil engineering, 16*(7), 818-836. doi:https://doi.org/10.1080/19648189.2012.672211

Baldi, A., & Bertolino, F. (2015). Experimental analysis of the errors due to polynomial interpolation in digital image correlation. *Strain, 51*(3), 248-263. doi:https://doi.org/10.1111/str.12137

Bigger, R., Blaysat, B., Boo, C., Grewer, M., Hu, J., Jones, A., . . . Schmidt, T. (2018). A good practices guide for digital image correlation. *Comput. Sci*.

Bing, P., Hui-Min, X., Bo-Qin, X., & Fu-Long, D. (2006). Performance of sub-pixel registration algorithms in digital image correlation. *Measurement science and technology*, *17*(6), 1615. doi:https://doi.org/10.1088/0957-0233/17/6/045

Bisby, L., Take, W., & Caspary, A. (2007). *Quantifying strain variation in FRP confined concrete using digital image correlation: Proof-of-concept and initial results.* Paper presented at the Asia-Pacific conference on FRP in structures (APFIS 2007). Dept of Civil Eng. Queen's University, Canada.

Biswal, S., & Ramaswamy, A. (2016). Measurement of existing prestressing force in concrete structures through an embedded vibrating beam strain gauge. *Measurement, 83*, 10-19. doi:https://doi.org/10.1016/j.measurement.2016.01.031

Blaber, J., Adair, B., & Antoniou, A. (2015). Ncorr: open-source 2D digital image correlation matlab software. *Experimental Mechanics*, *55*(6), 1105-1122. doi:https://doi.org/10.1007/s11340-015-0009-1

Bomarito, G., Hochhalter, J., Ruggles, T., & Cannon, A. (2017). Increasing accuracy and precision of digital image correlation through pattern optimization. *Optics and Lasers in Engineering*, *91*, 73-85. doi:https://doi.org/10.1016/j.optlaseng.2016.11.005

Bossuyt, S. (2013). Optimized patterns for digital image correlation *Imaging Methods for Novel Materials and Challenging Applications, Volume 3* (pp. 239-248): Springer.

Boulekbache, B., Hamrat, M., Chemrouk, M., & Amziane, S. (2015). Failure mechanism of fibre reinforced concrete under splitting test using digital image correlation. *Materials and structures*, *48*(8), 2713-2726. doi:https://DOI10.1617/s11527-014-0348-x

Bourcier, M., Bornert, M., Dimanov, A., Héripré, E., & Raphanel, J. (2013). Multiscale experimental investigation of crystal plasticity and grain boundary sliding in synthetic halite using digital image correlation. *Journal of Geophysical Research: solid earth*, *118*(2), 511-526. doi:https://doi.org/10.1002/jgrb.50065

Bruck, H., McNeill, S., Sutton, M. A., & Peters, W. (1989). Digital image correlation using Newton-Raphson method of partial differential correction. *Experimental Mechanics*, *29*(3), 261-267.

Caggegi, C., Sciuto, D., & Cuomo, M. (2018). Experimental study on effective bond length of basalt textile reinforced mortar strengthening system: Contributions of digital image correlation. *Measurement, 129*, 119-127. doi:https://doi.org/10.1016/j.measurement.2018.07.003

Chu, T., Ranson, W., & Sutton, M. A. (1985). Applications of digital-image-correlation techniques to experimental mechanics. *Experimental Mechanics*, *25*(3), 232-244.

Cintrón, R., & Saouma, V. (2008). Strain measurements with the digital image correlation system Vic-2D. *System*, *106*, 2D.

Corr, D., Accardi, M., Graham-Brady, L., & Shah, S. (2007). Digital image correlation analysis of interfacial debonding properties and fracture behavior in concrete. *Engineering Fracture Mechanics*, *74*(1-2), 109-121. doi:https://doi.org/10.1016/j.engfracmech.2006.01.035

Correlated Solutions. (2009). Vic-2D-2009-Guide.

Coșa, A., Hegheș, B., Negruțiu, C., & Kiss, Z. (2020). *Strain and Displacement Measurements in Reinforced Self-Compacting Concrete Beams with Openings Using Digital Image Correlation Technique.* Paper presented at the Multidisciplinary Digital Publishing Institute Proceedings.

Crammond, G., Boyd, S., & Dulieu-Barton, J. (2013). Speckle pattern quality assessment for digital image correlation. *Optics and Lasers in Engineering*, *51*(12), 1368-1378. doi:https://doi.org/10.1016/j.optlaseng.2013.03.014

Deng, L., & Zhao, R. (2013). A vibration analysis method based on hybrid techniques and its application to rotating machinery. *Measurement*, *46*(9), 3671-3682. doi:https://doi.org/10.1016/j.measurement.2013.07.014

Dong, Y., & Pan, B. (2017). A review of speckle pattern fabrication and assessment for digital image correlation. *Experimental Mechanics*, *57*(8), 1161-1181. doi:https://DOI10.1007/s11340-017-0283-1

Dutton, M., Take, W. A., & Hoult, N. A. (2014). Curvature monitoring of beams using digital image correlation. *Journal of Bridge Engineering*, *19*(3), 05013001. doi:https://doi.org/10.1061/(ASCE)BE.1943-5592.0000538

Eberl, C., Thompson, R., Gianola, D., & Bundschuh, S. (2006). Digital image correlation and tracking with Matlab. *Matlab Central file exchange*.

Fayyad, T. M., & Lees, J. M. (2014). Application of digital image correlation to reinforced concrete fracture. *Procedia Materials Science*, *3*, 1585-1590. doi:https://doi.org/10.1016/j.mspro.2014.06.256

Fayyad, T. M., & Lees, J. M. (2017). Experimental investigation of crack propagation and crack branching in lightly reinforced concrete beams using digital image correlation. *Engineering*

Fracture Mechanics, 182, 487-505. doi:https://doi.org/10.1016/j.engfracmech.2017.04.051

Gao, Z., Zhang, Q., Su, Y., & Wu, S. (2017). Accuracy evaluation of optical distortion calibration by digital image correlation. *Optics and Lasers in Engineering, 98*, 143-152. doi:https://doi.org/10.1016/j.optlaseng.2017.06.008

Gauvin, C., Jullien, D., Doumalin, P., Dupré, J. C., & Gril, J. (2014). Image correlation to evaluate the influence of hygrothermal loading on wood. *Strain, 50*(5), 428-435. doi:https://doi.org/10.1111/str.12090

Gehri, N., Mata-Falcón, J., & Kaufmann, W. (2020). Automated crack detection and measurement based on digital image correlation. *Construction and Building Materials, 256*, 119383. doi:https://doi.org/10.1016/j.conbuildmat.2020.119383

Gencturk, B., Hossain, K., Kapadia, A., Labib, E., & Mo, Y.-L. (2014). Use of digital image correlation technique in full-scale testing of prestressed concrete structures. *Measurement, 47*, 505-515. doi:https://doi.org/10.1016/j.measurement.2013.09.018

Górszczyk, J., Malicki, K., & Zych, T. (2019). Application of digital image correlation (DIC) method for road material testing. *Materials, 12*(15), 2349. doi:https://doi.org/10.3390/ma12152349

Granshaw, S. (1980). Bundle adjustment methods in engineering photogrammetry. *The Photogrammetric Record, 10*(56), 181-207. doi:https://doi.org/10.1111/j.1477-9730.1980.tb00020.x

Grediac, M. (2004). The use of full-field measurement methods in composite material characterization: interest and limitations. *Composites Part A: applied science and manufacturing, 35*(7-8), 751-761. doi:https://doi.org/10.1016/j.compositesa.2004.01.019

Hall, S. A., Bornert, M., Desrues, J., Pannier, Y., Lenoir, N., Viggiani, G., & Bésuelle, P. (2010). Discrete and continuum analysis of localised deformation in sand using X-ray μCT and volumetric digital image correlation. *Geotechnique, 60*(5), 315-322. doi:https://doi.org/10.1680/geot.2010.60.5.315

Hosseinzadeh, F., Yan, W., & Pierron, F. (2020). Recent advances in digital image correlation: A review with application to continuous wave and pulsed laser-based DIC. *Optics and Lasers in Engineering, 124, 105894.*

Hoult, N. A., Take, W. A., Lee, C., & Dutton, M. (2013). Experimental accuracy of two dimensional strain measurements using digital image correlation. *Engineering Structures, 46*, 718-726. doi:https://doi.org/10.1016/j.engstruct.2012.08.018

Hua, T., Xie, H., Wang, S., Hu, Z., Chen, P., & Zhang, Q. (2011). Evaluation of the quality of a speckle pattern in the digital image correlation method by mean subset fluctuation. *Optics & Laser Technology, 43*(1), 9-13. doi:https://doi.org/10.1016/j.optlastec.2010.04.010

Huang, Z., Tu, Y., Meng, S., Sabau, C., Popescu, C., & Sas, G. (2019). Experimental study on shear deformation of reinforced concrete beams using digital image correlation. *Engineering Structures, 181*, 670-698. doi:https://doi.org/10.1016/j.engstruct.2018.12.056

Hung, P.-C., & Voloshin, A. (2003). In-plane strain measurement by digital image correlation. *Journal of the Brazilian Society of Mechanical Sciences and Engineering, 25*, 215-221. doi:https://doi.org/10.1590/S1678-58782003000300001

Kozicki, J., & Tejchman, J. (2007). Experimental investigations of strain localization in concrete using Digital Image Correlation (DIC) technique. *Archives of Hydro-Engineering and Environmental Mechanics, 54*(1), 3-24.

Lakavath, C., Joshi, S. S., & Prakash, S. S. (2019). Investigation of the effect of steel fibers on the shear crack-opening and crack-slip behavior of prestressed concrete beams using digital image correlation. *Engineering Structures, 193*, 28-42. doi:https://doi.org/10.1016/j.engstruct.2019.05.030

Lecompte, D., Smits, A., Bossuyt, S., Sol, H., Vantomme, J., Van Hemelrijck, D., & Habraken, A. (2006). Quality assessment of speckle patterns for digital image correlation. *Optics and Lasers in Engineering, 44*(11), 1132-1145. doi:https://doi.org/10.1016/j.optlaseng.2005.10.004

Lehoucq, R. B., Reu, P. L., & Turner, D. Z. (2015). A novel class of strain measures for digital image correlation. *Strain, 51*(4), 265-275. doi:https://doi.org/10.1111/str.12138

Li, D., Huang, P., Chen, Z., Yao, G., Guo, X., Zheng, X., & Yang, Y. (2020). Experimental study on fracture and fatigue crack propagation processes in concrete based on DIC technology. *Engineering Fracture Mechanics, 235*, 107166. doi:https://doi.org/10.1016/j.engfracmech.2020.107166

Lionello, G., & Cristofolini, L. (2014). A practical approach to optimizing the preparation of speckle patterns for digital-image correlation. *Measurement science and technology, 25*(10), 107001. doi:https://doi.org/10.1088/0957-0233/25/10/107001

Liu, X.-Y., Li, R.-L., Zhao, H.-W., Cheng, T.-H., Cui, G.-J., Tan, Q.-C., & Meng, G.-W. (2015).

Quality assessment of speckle patterns for digital image correlation by Shannon entropy. *Optik, 126*(23), 4206-4211. doi:https://doi.org/10.1016/j.ijleo.2015.08.034

Liu, Y., Dong, B., Bai, Y., Xu, J., Zhang, Y., Ye, S., & Zhou, Y. (2015). Perspective Measurement of the Out-of-plane Displacement and Normal Strain Field Distributions Inside Glass Fibre-reinforced Resin Matrix Composite. *Strain, 51*(3), 198-205. doi:https://doi.org/10.1111/str.12133

Lugli, P. (2009). *Spray-coating deposition for large area organic thin-film devices.* Paper presented at the Technical proceedings of the 2009 NSTI Nanotechnology Conference and Expo: Nanotech Conference & Expo 2009; Volume 2.

Mazzoleni, P., Zappa, E., Matta, F., & Sutton, M. A. (2015). Thermo-mechanical toner transfer for high-quality digital image correlation speckle patterns. *Optics and Lasers in Engineering, 75*, 72-80. doi:https://doi.org/10.1016/j.optlaseng.2015.06.009

McCormick, N., & Lord, J. (2010). Digital image correlation. *Materials today, 13*(12), 52-54. doi:https://doi.org/10.1016/S1369-7021(10)70235-2

McCormick, N., & Lord, J. (2012). *Digital image correlation for structural measurements.* Paper presented at the Proceedings of the Institution of Civil Engineers-Civil Engineering.

Mohan, A., & Poobal, S. (2018). Crack detection using image processing: A critical review and analysis. *Alexandria Engineering Journal, 57*(2), 787-798.

Neggers, J., Blaysat, B., Hoefnagels, J. P., & Geers, M. G. (2016). On image gradients in digital image correlation. *International Journal for Numerical Methods in Engineering, 105*(4), 243-260. doi:https://doi.org/10.1002/nme.4971

Ottman, N., Ruokolainen, L., Suomalainen, A., Sinkko, H., Karisola, P., Lehtimäki, J., . . . Fyhrquist, N. (2019). Soil exposure modifies the gut microbiota and supports immune tolerance in a mouse model. *Journal of allergy and clinical immunology, 143*(3), 1198-1206. e1112. doi:https://doi.org/10.1016/j.jaci.2018.06.024

Pan, B. (2011). Recent progress in digital image correlation. *Experimental Mechanics, 51*(7), 1223-1235. doi:https://doi.org//10.1007/s11340-010-9418-3

Pan, B. (2014). An evaluation of convergence criteria for digital image correlation using inverse compositional Gauss–Newton algorithm. *Strain, 50*(1), 48-56. doi:https://doi.org/10.1111/str.12066

Pan, B., & Li, K. (2011). A fast digital image correlation method for deformation measurement. *Optics and Lasers in Engineering, 49*(7), 841-847. doi:https://doi.org/10.1016/j.optlaseng.2011.02.023

Pan, B., Li, K., & Tong, W. (2013). Fast, robust and accurate digital image correlation calculation without redundant computations. *Experimental Mechanics, 53*(7), 1277-1289. doi:https://doi.org/10.1007/s11340-013-9717-6

Pan, B., Lu, Z., & Xie, H. (2010). Mean intensity gradient: an effective global parameter for quality assessment of the speckle patterns used in digital image correlation. *Optics and Lasers in Engineering, 48*(4), 469-477. doi:https://doi.org/10.1016/j.optlaseng.2009.08.010

Pan, B., Qian, K., Xie, H., & Asundi, A. (2009). Two-dimensional digital image correlation for in-plane displacement and strain measurement: a review. *Measurement science and technology, 20*(6), 062001. doi:https://doi.org/10.1088/0957-0233/20/6/062001

Pan, B., Tian, L., & Song, X. (2016). Real-time, non-contact and targetless measurement of vertical deflection of bridges using off-axis digital image correlation. *Ndt & E International, 79*, 73-80. doi:https://doi.org/10.1016/j.ndteint.2015.12.006

Pan, B., & Wang, B. (2016). Digital image correlation with enhanced accuracy and efficiency: a comparison of two subpixel registration algorithms. *Experimental Mechanics, 56*(8), 1395-1409. doi:hhtp://doi.org/10.1007/s11340-016-0180-z

Pan, B., Xie, H., & Wang, Z. (2010). Equivalence of digital image correlation criteria for pattern matching. *Applied optics, 49*(28), 5501-5509. doi:https://doi.org/10.1364/ao.49.005501 10.1364/ao.49.005501

Pan, B., Xie, H., Wang, Z., Qian, K., & Wang, Z. (2008). Study on subset size selection in digital image correlation for speckle patterns. *Optics express, 16*(10), 7037-7048. doi:https://doi.org/10.1364/OE.16.007037

Pérez, V. Q., Prieto, D. C., & Orduz, L. E. Z. (2021). Mechanical characterization of self-compacting steel fiber reinforced concrete using digital image correlation. *Engineering Fracture Mechanics, 246*, 107618. doi:https://doi.org/10.1016/j.engfracmech.2021.107618

Peters, W., & Ranson, W. (1982). Digital imaging techniques in experimental stress analysis. *Optical engineering, 21*(3), 213427. doi:https://doi.org/10.1117/12.7972925

Peters, W., Ranson, W., Sutton, M., Chu, T., & Anderson, J. (1983). Application of digital correlation methods to rigid body mechanics. *Optical engineering, 22*(6), 226738. doi:https://doi.org/10.1117/12.7973231

PI, L. Y., Smith, L., Gothekar, M. A., & Chen, M. X. (2010). Measure Strain Distribution Using Digital Image Correlation (DIC) for Tensile Tests.

Quanjin, M., Rejab, M., Halim, Q., Merzuki, M., & Darus, M. (2020). Experimental investigation of the tensile test using digital image correlation (DIC) method. *Materials Today: Proceedings*, *27*, 757-763. doi:https://doi.org/10.1016/j.matpr.2019.12.072

Ramos, T., Braga, D. F., Eslami, S., Tavares, P. J., & Moreira, P. (2015). Comparison between finite element method simulation, digital image correlation and strain gauges measurements in a 3-point bending flexural test. *Procedia Engineering*, *114*, 232-239. doi:https://doi.org/10.1016/j.proeng.2015.08.063

Ranson, W., Sutton, M., & Peters, W. (1987). Holographic and laser speckle interferometry. *Handbook of Experimental Mechanics*, 388-429.

Rayan, M. K. (2008). Spray deposition of biomolecular thin films.

Reu, P. (2014a). All about speckles: aliasing. *Experimental techniques*, *38*(5), 1-3. doi:https://doi.org/10.1111/ext.12111

Reu, P. (2014b). All about speckles: speckle size measurement. *Experimental techniques*, *38*(6), 1-2. doi:https://doi.org/10.1111/ext.12110

Reu, P. (2015a). All about speckles: contrast. *Experimental techniques*, *39*(1), 1-2. doi:https://doi.org/10.1111/ext.12126

Reu, P. (2015b). All about speckles: edge sharpness. *Experimental techniques*, *39*(2), 1-2. doi:https://doi.org/10.1111/ext.12139

Reu, P. L., Toussaint, E., Jones, E., Bruck, H. A., Iadicola, M., Balcaen, R., . . . Simonsen, M. (2018). DIC challenge: developing images and guidelines for evaluating accuracy and resolution of 2D analyses. *Experimental Mechanics*, *58*(7), 1067-1099. doi:https://doi.org/10.1007/s11340-017-0349-0

Sebastian, C., & Patterson, E. (2015). Calibration of a digital image correlation system. *Experimental techniques*, *39*(1), 21-29. doi:https://doi.org/10.1111/ext.12005

Seo, B. H., Kim, J. H., Park, J. B., & Jung, G. D. (2015). Crack propagation characteristics of particulate reinforced composites using digital image correlation: Charakterisierung der Rissausbreitung von partikelverstärkten Verbundwerkstoffen mittels digitaler Bildkorrelation. *Materialwissenschaft und Werkstofftechnik*, *46*(4-5), 387-393. doi:https://doi.org/10.1002/mawe.201500413

Shah, S., & Kishen, J. C. (2011). Fracture properties of concrete–concrete interfaces using digital image correlation. *Experimental Mechanics*, *51*(3), 303-313. doi:https://doi.org/10.1007/s11340-010-9358-y

Shukla, N., & Mishra, M. K. (2018). Digital Image Correlation Techniques for Experimental Strain Analysis: A Review.

Skarżyński, Ł., Kozicki, J., & Tejchman, J. (2013). Application of DIC technique to concrete—study on objectivity of measured surface displacements. *Experimental Mechanics*, *53*(9), 1545-1559. doi:https://doi.org/10.1007/s11340-013-9781-y

Skarżyński, Ł., Syroka, E., & Tejchman, J. (2011). Measurements and calculations of the width of the fracture process zones on the surface of notched concrete beams. *Strain*, *47*, e319-e332. doi:https://doi.org/10.1111/j.1475-1305.2008.00605.x

Stoilov, G., Kavardzhikov, V., & Pashkouleva, D. (2012). A comparative study of random patterns for digital image correlation. *Journal of Theoretical and Applied Mechanics*, *42*(2), 55. doi:https://doi.org/10.2478/v10254-012-0008-x

Su, M.-N., Young, B., & Gardner, L. (2016). The continuous strength method for the design of aluminium alloy structural elements. *Engineering Structures*, *122*, 338-348. doi:https://doi.org/10.1016/j.engstruct.2016.04.040

Su, Y., Gao, Z., Zhang, Q., & Wu, S. (2018). Spatial uncertainty of measurement errors in digital image correlation. *Optics and Lasers in Engineering*, *110*, 113-121. doi:https://doi.org/10.1016/j.optlaseng.2018.05.016

Su, Y., Zhang, Q., Fang, Z., Wang, Y., Liu, Y., & Wu, S. (2019). Elimination of systematic error in digital image correlation caused by intensity interpolation by introducing position randomness to subset points. *Optics and Lasers in Engineering*, *114*, 60-75. doi:https://doi.org/10.1016/j.optlaseng.2018.10.012

Sutton, M., Mingqi, C., Peters, W., Chao, Y., & McNeill, S. (1986). Application of an optimized digital correlation method to planar deformation analysis. *Image and Vision Computing*, *4*(3), 143-150. doi:https://doi.org/10.1016/0262-8856(86)90057-0

Sutton, M. A., Orteu, J. J., & Schreier, H. (2009). *Image correlation for shape, motion and deformation measurements: basic concepts, theory and applications*: Springer Science & Business Media.

Syed, Y., Saliba, J., & Loukili, A. (2013). *Study of evolution of fracture process zone in concrete by simultaneous application of digital image correlation and acoustic emission.* Paper presented at the VIII International Conference on Fracture Mechanics of Concrete and Concrete Structures FraMCoS-8.

Tejchman, J. (2010). Calculations of fracture process zones on meso-scale in notched concrete beams subjected to three-point bending. *European Journal of Mechanics-A/Solids*, *29*(4), 746-760. doi:https://doi.org/10.1016/j.euromechsol.2010.02.008

Tekieli, M., De Santis, S., de Felice, G., Kwiecień, A., & Roscini, F. (2017). Application of Digital Image Correlation to composite reinforcements testing. *Composite Structures*, *160*, 670-688. doi:https://doi.org/10.1016/j.compstruct.2016.10.096

Valença, J., Dias-da-Costa, D., & Júlio, E. (2012). Characterisation of concrete cracking during laboratorial tests using image processing. *Construction and Building Materials*, *28*(1), 607-615. doi:https://doi.org/10.1016/j.conbuildmat.2011.08.082

Valença, J., Júlio, E., & Araújo, H. (2012). Applications of photogrammetry to structural assessment. *Experimental techniques*, *36*(5), 71-81. doi:https://doi.org/10.1111/j.1747-1567.2011.00731.x

Van Den Heuvel, F., Kroon, R., & Le Poole, R. (1993). Digital close-range photogrammetry using artificial targets. *International Archives of Photogrammetry and Remote Sensing*, *29*, 222-222.

Verbruggen, S., Aggelis, D. G., Tysmans, T., & Wastiels, J. (2014). Bending of beams externally reinforced with TRC and CFRP monitored by DIC and AE. *Composite Structures*, *112*, 113-121. doi:https://doi.org/10.1016/j.compstruct.2014.02.006

Wang, J. J., Gowripalan, N., Li, J., & Nguyen, V. V. (2019). Close-range photogrammetry for accurate deformation distribution measurement *Mechanics of Structures and Materials XXIV* (pp. 822-829): CRC Press.

Wang, Y., Sutton, M., Bruck, H., & Schreier, H. (2009). Quantitative error assessment in pattern matching: effects of intensity pattern noise, interpolation, strain and image contrast on motion measurements. *Strain*, *45*(2), 160-178. doi:https://doi.org/10.1111/j.1475-1305.2008.00592.x

Wattrisse, B., Chrysochoos, A., Muracciole, J.-M., & Némoz-Gaillard, M. (2001). Analysis of strain localization during tensile tests by digital image correlation. *Experimental Mechanics*, *41*(1), 29-39. doi:https://doi.org/10.1007/BF02323101

White, D., Take, W., & Bolton, M. (2003). Soil deformation measurement using particle image velocimetry (PIV) and photogrammetry. *Geotechnique*, *53*(7), 619-631. doi:https://doi.org/10.1680/geot.2003.53.7.619

Williams, H. E. (2001). On introducing engineering strain. *International Journal of Mechanical Engineering Education*, *29*(4), 397-403. doi:https://doi.org/10.7227/IJMEE.29.4.9

Xie, Z., Zhou, H., Lu, L., & Chen, Z. (2017). An investigation into fracture behavior of geopolymer concrete with digital image correlation technique. *Construction and Building Materials*, *155*, 371-380. doi:https://doi.org/10.1016/j.conbuildmat.2017.08.041

Yaofeng, S., & Pang, J. H. (2007). Study of optimal subset size in digital image correlation of speckle pattern images. *Optics and Lasers in Engineering*, *45*(9), 967-974. doi:https://doi.org/10.1016/j.optlaseng.2007.01.012

Zhao, J., Sang, Y., & Duan, F. (2019). The state of the art of two-dimensional digital image correlation computational method. *Engineering reports*, *1*(2), e12038. doi: https://doi.org/10.1002/eng2.12038

Zhao, P., Zsaki, A. M., & Nokken, M. R. (2018). Using digital image correlation to evaluate plastic shrinkage cracking in cement-based materials. *Construction and Building Materials*, *182*, 108-117. doi:https://doi.org/10.1016/j.conbuildmat.2018.05.239

Zhou, P., & Goodson, K. E. (2001). Subpixel displacement and deformation gradient measurement using digital image/speckle correlation. *Optical engineering*, *40*(8), 1613-1620. doi:https://doi.org/10.1117/1.1387992

Zhuang, X. Y., Chen, L., Komarneni, S., Zhou, C. H., Tong, D. S., Yang, H. M., . . . Wang, H. (2016). Fly ash-based geopolymer: clean production, properties and applications. *Journal of Cleaner Production*, *125*, 253-267. doi:https://doi.org/10.1016/j.jclepro.2016.03.019